July 1, 1997

Local multiplicity fluctuations in hadronic Z decay

The L3 Collaboration

Abstract

Local multiplicity fluctuations in hadronic Z decays are studied using the L3 detector at LEP. In addition to the normalised-factorial-moment method, fluctuations are studied for the first time by means of bunching parameters. Fluctuations in rapidity calculated with respect to the thrust axis are found to exhibit genuine multifractal fluctuations. Fluctuations are also studied in the four-momentum difference of two particles. Monte Carlo models, which have been tuned to reproduce global event-shape distributions and single-particle inclusive distributions, are found to be unable to describe the local multiplicity fluctuations.

Submitted to *XVIII International Symposium on Lepton-Photon Interactions*

1 Introduction

Hadronic final states of e^+e^- collisions provide a favourable environment for QCD studies. Initially, the hadronic system is simply a quark-antiquark pair. The process by which this $q\overline{q}$ pair develops into hadrons is usually described by a parton shower followed by hadronisation and resonance decays, including the effects of Bose-Einstein (BE) interference. At present, only the parton shower can be reliably calculated in QCD. Monte Carlo programs incorporating the QCD parton shower and phenomenological models of hadronisation and resonance decay have been successful in describing global features. However, more detailed comparisons, such as correlations in restricted regions of phase space, have revealed discrepancies.

In this paper we use high statistics data from the L3 experiment at LEP to study correlations in terms of fluctuations in the charged particle multiplicity distribution in restricted regions of phase space as a function of the size of the region. While the study of the multiplicity distribution in full phase space deals with limited dynamical information, being mainly influenced by charge and energy-momentum conservation, the investigation of the evolution of the multiplicity distribution with decreasing size of local phase space windows (bins), can provide detailed information on hadron production without these trivial constraints. Physical processes underlying such short-range correlations include jet structure, string or cluster fragmentation, resonance decays and Bose-Einstein interference. A deviation of this local multiplicity distribution from the Poissonian expected for purely independent particle production measures dynamical local multiplicity fluctuations, which are a consequence of short-range correlations between final-state particles.

Fluctuations are often studied using the normalised factorial moments (NFMs) of the local multiplicity distribution, $P_n(\delta)$, which is the probability to find n particles inside a restricted phase space bin of size δ [1]. The NFM of order q, $F_q(\delta)$, is defined by

$$F_q(\delta) \quad = \quad \frac{\langle n^{[q]}\rangle}{\langle n\rangle^q}\,, \tag{1}$$

$$\langle n^{[q]}\rangle = \sum_{n=q}^{\infty} n^{[q]} P_n(\delta)\,, \qquad n^{[q]} = n(n-1)\ldots(n-q+1)\,. \tag{2}$$

If $P_n(\delta)$ is a Poisson distribution, $F_q(\delta) = 1$ for all q. If there are fluctuations, F_q deviates from unity. Further, if the fluctuations are self-similar, $F_q(\lambda\delta) = \lambda^{-\phi_q} F_q(\delta)$, and a power-like increase emerges with decreasing δ, $F_q(\delta) \propto \delta^{-\phi_q}$, where $\phi_q = (q-1)d_q$, and d_q are the anomalous fractal dimensions. Local fluctuations are classified as monofractal (d_q is independent of q) or multifractal (d_q is a function of q). (See recent reviews [2]).

Local fluctuations in e^+e^--processes have been studied in several experiments [3–11]. The data do exhibit an approximate power-like rise of the NFMs with decreasing δ, especially when evaluated in two- and three-dimensional phase space variables. All four LEP experiments have found that current Monte Carlo models can, in general, describe the NFMs, even without additional tuning. Important exceptions have, however, been found in rapidity defined with respect to the sphericity axis by DELPHI [9] (for restricted charge-multiplicity and p_T regions) and by OPAL. [7]

2 Methods

Recently, it has been realized that the factorial moment method poorly reflects the information on local fluctuations, since the NFM of order q contains a contamination from lower-order correlation functions [2]. As a result, the nature of the fluctuations is difficult to determine from the behaviour of the NFMs. The fact that subtle details in the behaviour of $P_n(\delta)$ are lost, together with the small statistics used in previous analyses, may be the reason why different Monte Carlo models have succeeded in reasonably describing the local fluctuations measured in e^+e^- annihilation.

Factorial moments also suffer from a statistical bias due to the finite size of the event sample, which becomes more severe as δ decreases or q increases. This is because in actual measurements the NFMs are determined by the first few terms of expression (2). In most cases this leads to a significant underestimate of the measured NFMs with respect to their true values [12].

While cumulants are a more sensitive statistical tool (see [2] and references therein), their measurement is rather difficult and has rarely been attempted. Besides, the cumulants are expected to have an even larger statistical bias.

An alternative to the NFMs and their cumulants is provided by bunching parameters (BPs), η_q, [13,14] defined by

$$\eta_q(\delta) = \frac{q}{q-1}\frac{P_q(\delta)\,P_{q-2}(\delta)}{P^2_{q-1}(\delta)}, \qquad q = 2, 3, \ldots, \tag{3}$$

which are more sensitive than the NFMs to the variation in the shape of $P_n(\delta)$ with decreasing δ. In the case of self-similar fluctuations, one expects $\eta_2(\delta) \propto \delta^{-d_2}$. For multifractal local fluctuations, the $\eta_q(\delta)$ are δ-dependent functions for all $q \geq 3$, while for monofractal behaviour $\eta_q(\delta)$ is independent of δ for $q \geq 3$ [13]. For independent particle production, the BPs are δ-independent constants (for a Poisson distribution, $\eta_q(\delta) = 1$).

From an experimental point of view, the BPs have important advantages [14]: (1) They are less severely affected by statistical bias than the NFMs, since the qth-order BP resolves only the behaviour of the multiplicity distribution near multiplicity $n = q-1$; (2) for the calculation of the BP of order q, one only needs to be able to resolve q particles in a bin, rather than all particles as for the NFMs; and (3) many systematic errors cancel in the ratio of probabilities.

In order to reduce the statistical error we use the bin-averaged "horizontal" NFMs [1] and BPs [13,14]: The NFM of order q is calculated using the standard definition:

$$F_q(M) = \frac{1}{M}\sum_{m=1}^{M}\frac{\langle n_m^{[q]}\rangle}{\langle \bar{n}\rangle^q}, \qquad n_m^{[q]} = n_m(n_m-1)\ldots(n_m-q+1), \tag{4}$$

where n_m is the number of particles in bin m, $\langle \bar{n}\rangle = \bar{N}/M$, $\bar{N}$ is the average multiplicity for full phase space, $M = \Delta/\delta$ is the total number of bins, and Δ represents the full phase space volume. The horizontal BP of order q is calculated using

$$\eta_q(M) = \frac{q}{q-1}\frac{\bar{N}_q(M)\,\bar{N}_{q-2}(M)}{\bar{N}^2_{q-1}(M)}, \qquad \bar{N}_q(M) = \frac{1}{M}\sum_{m=1}^{M} N_q(m,\delta)\,, \tag{5}$$

where $N_q(m,\delta)$ is the number of events having q particles in bin m and M has the same meaning as for the NFMs.

Note that bin-averaging, as used in the above definitions, is only justified for a flat single-particle density distribution. To be able to study non-flat distributions, we transform the original phase space variable to one in which the underlying density is (approximately) uniform, as suggested by Białas, Gazdzicki and Ochs [15].

When defined in this way, the NFMs and BPs both require dividing phase space into a number of bins. This has the disadvantage of losing information on local fluctuations in particle density ("spikes") that are divided by bin boundaries. Recently a new type of bunching parameter has been proposed [14], which can be used to study the fluctuation of the number of spikes (defined below) per event. Generalized integral bunching parameters are defined by

$$\chi_q(\epsilon) = \frac{q}{q-1} \frac{\Pi_q(\epsilon)\,\Pi_{q-2}(\epsilon)}{\Pi^2_{q-1}(\epsilon)}, \tag{6}$$

where $\Pi_q(\epsilon)$ is the probability of an event to have q spikes of size less than ϵ, irrespective of how many particles are inside each spike. For purely independent particle production, with the multiplicity distribution characterised by a Poissonian law, $\chi_q(\epsilon) = 1$ for all q.

To define the number of spikes of size less than ϵ, we need both a measure of the size of a spike and a method of assigning particles to spikes. For the size we choose to use the so-called Grassberger-Hentschel-Procaccia counting topology [16] for which the size is given by the maximum of all pairwise distances between particles in the spike. As distance between particles i and j we use the squared four-momentum difference $Q^2_{ij} = -(p_i - p_j)^2$. Spikes are then defined in the following way: Consider all possible combinations of two or more particles. For each combination the spike size is determined. If this size is larger than some maximum, ϵ, the combination is discarded. Of the remaining combinations, those completely contained in another (larger) combination are also discarded. Combinations left after this procedure are called spikes (of size less than ϵ). Note that while the assignment of particles to spikes is not unique (the same particle can be in more than one spike), the number of spikes is unambiguously defined.

The BPs are then given by

$$\chi_q(Q^2) = \frac{q}{q-1} \frac{S_q(Q^2)\,S_{q-2}(Q^2)}{S^2_{q-1}(Q^2)}, \tag{7}$$

where $S_q(Q^2)$ is the number of events having q spikes of size less than Q^2.

3 Data Samples and Analysis Procedures

We use data, corresponding to an integrated luminosity of 47 pb^{-1}, collected by L3 [17] at a centre of mass energy of $\sqrt{s} \simeq 91.2$ GeV during the 1994 LEP running period. Hadronic events are selected using (1) energy deposits in the electromagnetic and hadronic calorimeters, and (2) momenta measured in the Central Tracking Detector (TEC) and the Silicon Microvertex Detector (SMD).

First, a loose calorimeter-based selection is performed in order to reject non-hadronic background. Using clusters with energy larger than 100 MeV, we require

$$0.6 < \frac{E^{\mathrm{C}}}{\sqrt{s}} < 1.4, \qquad \frac{E_\perp}{E^{\mathrm{C}}} < 0.4, \qquad \frac{E_\parallel}{E^{\mathrm{C}}} < 0.4, \qquad 13 < N_{\mathrm{cl}} < 75,$$

where E^{C} is the total energy observed in the calorimeters, $E_\perp$ ($E_\parallel$) is the energy imbalance in the plane perpendicular (parallel) to the beam direction, and N_{cl} is the number of calorimeter clusters. To ensure that the event is contained in the barrel region of the calorimeters we require $|\cos\theta_{\mathrm{thr}}| < 0.74$, where θ_{thr} is the polar angle of the event thrust axis.

To obtain a sample with well-measured charged tracks, a further selection is performed using only tracks which have passed certain quality cuts. The distance of closest approach (projected onto the transverse plane) of a track to the nominal interaction vertex is required to be less than 5 mm and its transverse momentum must be larger than 100 MeV. To ensure that the event lies within the full acceptance of the TEC and SMD, the direction of the thrust axis, as determined from the charged tracks, must satisfy $|\cos\theta_{\mathrm{thr}}| < 0.7$. Events are then selected using criteria similar to the above calorimeter-based selection, but using tracks:

$$\frac{\sum_i p_i}{\sqrt{s}} > 0.15, \qquad \frac{\left|\sum_i p_{\|i}\right|}{\sum_i p_i} < 0.75, \qquad \frac{\left|\sum_i \vec{p}_{\perp i}\right|}{\sum_i p_i} < 0.75, \qquad N_{\mathrm{ch}} > 4,$$

where p_i is the momentum of particle i and the sum runs over all tracks of an event, and where N_{ch} is the number of charged tracks. The resulting sample contains about 810k events.

The results are corrected for selection and acceptance losses. To determine the corrections, a Monte Carlo sample of hadronic events is generated with JETSET including initial-state photon radiation. On the first (generator) level, the sample contains all charged final-state particles with a lifetime greater than 10^{-9} s. On the second (detector) level, it includes distortions due to detector effects, such as particle interactions and decays in the detector, resolution and acceptance. These effects are simulated using the GEANT3 [18] and GHEISHA [19] programs. Furthermore, time-dependent variations of the detector response have been introduced based on continuous detector monitoring and calibration. These Monte Carlo events were reconstructed with the same program as the data and passed through the same selection procedure.

In Fig. 1 we show distributions of the single-particle rapidity with respect to the thrust axis, y, and the square of the pairwise four-momentum difference, Q^2, before correction for detector effects compared to the expected distributions from JETSET after detector simulation. It is in these variables, y and Q^2, that we study fluctuations in this paper. The comparisons are good, which indicates the quality of both the detector simulation and the JETSET predictions. It should be noted that these distributions are not used in the tuning of JETSET's parameters.

An NFM or BP corrected for detector effects, D_q^{cor}, is found by multiplying the value calculated directly from the data, D_q^{raw}, by a correction factor $C_q = M_q^{\mathrm{gen}}/M_q^{\mathrm{det}}$, where, M_q^{gen} and M_q^{det} are the corresponding NFM or BP calculated from the generator- and detector-level Monte Carlo samples, respectively. These corrections, which tend to be larger for smaller bin size, are in no case larger than about 15% [20].

To reduce possible systematic bias, the minimum bin size is chosen comparable to the experimental resolution, which was estimated [20, 21] by Monte Carlo simulation. In the case of Q^2, the smallest bin size is large enough that the measurements are not strongly affected by Dalitz decays ($\pi^0 \to e^+e^-\gamma$) or by photon conversions.

The error bars on the results include contributions from both statistical and systematic errors on the raw quantities and on the correction factors. The statistical errors on the $F_q(M)$ and $\eta_q(M)$ are derived from the covariance matrix of the NFMs and BPs. The statistical errors for the generalised integral BPs are derived according to the expression obtained in [14]. Systematic errors on the raw quantities have been estimated by varying the event and track selection criteria. In calculating the statistical error for the correction factor, we assume that the errors for the generator-level and detector-level Monte Carlo's are independent. This assumption leads to an upper limit of the error derived for C_q. As systematic error, we take half of the difference between the correction factors determined using JETSET and those using HERWIG. It is found that the correction factors C_q have a non-linear behaviour and, in general, tend to reduce the measured NFMs. OPAL has reported similar behaviour of the correction factors [7]. For small bin size, the total error is dominated by the systematic error on the correction factors.

The predictions of the JETSET 7.4 PS [22], ARIADNE 4.08 [23] and HERWIG 5.9 [24] models, all of which have been tuned to reproduce global event-shape and single-particle inclusive distributions [10, 25], are compared to the data. The errors on the JETSET predictions include both statistical and systematic errors. The systematic errors were estimated by varying, by one standard deviation, the JETSET parameters tuned by L3 [10, 25]: the Lund fragmentation function parameter b, the width of the Gaussian p_x and p_y hadronic transverse momentum distribution, and the value of Λ used for α_s in parton showers. The errors on the Monte Carlo results are dominated by the systematic errors. The errors (not shown) on the ARIADNE results are comparable to those on JETSET, while those of HERWIG are about 50% larger.

4 Results

4.1 Rapidity with respect to the thrust axis, y

To study fluctuations inside jets, we first determine the thrust axis and analyse the NFMs and BPs in the full rapidity range $|y| \leq 5$. Since the single-particle y distribution is non-uniform, we carry out the Białas-Gazdzicki-Ochs transformation before calculating the NFMs and BPs.

The horizontally normalised NFMs are shown in Fig. 2 as a function of the number of bins, M, in the transformed rapidity. They rise with increasing M and then saturate. Both JETSET and ARIADNE overestimate the NFMs for large M. This discrepancy increases with rising moment order q. HERWIG gives a reasonable description of the data.

BE correlations are an obvious candidate for the origin of local fluctuations in three-momentum phase space. To demonstrate the effect of BE correlations, the predictions of JETSET without BE interference*) are also shown in Fig. 2. It is seen that without the BE effect the NFMs rise more slowly and that the description of the data is only slightly worse than that of HERWIG, which also contains no BE interference.

Fig. 3 shows the results for the horizontally normalised BPs. The second-order BP decreases with increasing M up to $M \approx 40$, which is found to correspond to the value of M at which the maximum of the multiplicity distribution $P_n(\delta)$ first occurs at $n = 0$. All higher-order ($q > 2$) BPs show an approximate power-law increase with increasing M, indicating that the fluctuations in y are multifractal.

Disagreement with both JETSET and ARIADNE is observed for BPs of order 2 and 3, while higher-order BPs are described well. A direct comparison of the multiplicity distributions with Monte Carlo predictions is shown in Fig. 4 for the rapidity intervals $\delta y = 1.0$, 0.5, and 0.1 ($M = 10$, 20, 100). We see that the absolute disagreement is largest for low multiplicities and decreases with increasing multiplicity. However, the relative disagreement increases with multiplicity and tends to cancel in the higher-order BPs.

The values of η_2 decrease for JETSET when BE interference is not included, and agreement for higher orders is reasonable. HERWIG shows larger disagreement for the BPs even though it agreed well with the NFMs in Fig. 2. In particular, HERWIG greatly overestimates η_2. Since for small phase space cells, the second-order BP is related to the width of the distribution [13, 14], this means that HERWIG's local multiplicity distributions are too broad. This agrees with ALEPH's conclusion from a direct measurement of the dispersion for various (large) intervals of rapidity [26], but stresses the importance of the low values of n in this discrepancy.

*) The parameters of JETSET were retuned with BE interference disabled. This resulted in changes of PARJ(21), PARJ(42), and PARJ(81) from 0.411, 0.886, and 0.311 to 0.343, 1.1, and 0.312, respectively.

To study the disagreement between the data and Monte Carlo models in more detail, we split η_2 into two components:

$$\eta_2(M) = \eta_2^{(\pm\pm)}(M) + \eta_2^{(+-)}(M). \tag{8}$$

where $\eta_2^{(\pm\pm)}(M)$ is defined according to (5), but with $N_2(m,\delta)$ replaced by $N_2^{(\pm\pm)}(m,\delta)$, the number of events having two like-charged particles inside bin m of size δ. Analogously, $\eta_2^{(+-)}(M)$ is constructed from the number of events having two oppositely charged particles in the bin. Note that for combinatorial reasons, $\eta_2^{(\pm\pm)}(M) < \eta_2^{(+-)}(M)$. However, both would be independent of M in the case of independent production.

Fig. 5 shows that $\eta_2^{(\pm\pm)}(M)$ and $\eta_2^{(+-)}(M)$ indeed behave completely differently. While $\eta_2^{(\pm\pm)}(M)$ shows the expected rise (and saturation of the data at large M), $\eta_2^{(+-)}(M)$ shows a strong decrease at low M and the onset of an increase at large M. The structure of $\eta_2(M)$ observed in Fig. 3 is a combination of these two effects.

The BE modelling strongly affects the value of $\eta_2^{(\pm\pm)}(M)$, but the variation of $\eta_2^{(\pm\pm)}(M)$ with M seems to be due to other sources. The large error bars on the data are mainly systematical due to the generator dependence of the correction factors. The errors on the JETSET predictions (shaded areas) are dominantly systematic. They are mainly due to the uncertainty on the parameter responsible for the width of the Gaussian hadronic transverse momentum distribution in the Lund model. This shows the importance of fragmentation for the local quantity measured. Another observation is that the Monte Carlo overestimates the fluctuations for both like- and unlike-charged particle combinations at large M. The variation of JETSET fragmentation parameters has little influence on the unlike-charged particle fluctuations, but the BE modelling does have a significant influence on both the like- and unlike-charged particles.

The strong anti-bunching tendency (decrease of η_q with increasing M) seen for unlike-charged particles for $M \lesssim 20$ would be expected from chain-like particle production along the thrust axis, as expected from a QCD string model [27]. However, we observe that HERWIG as well as JETSET and ARIADNE exhibit this behaviour. Resonance decays are therefore a more likely explanation. Their decay particles tend to be of opposite charge and are typically separated in rapidity by $\delta y \sim 0.5$–1.0. As a result, a rapidity separation of this order of magnitude is more frequent between unlike-charged particles than between like-charged and $\eta_2^{(+-)}(M)$ is larger than $\eta_2^{(\pm\pm)}(M)$ at small M (large δy). However, this difference decreases rapidly with decreasing δy, disappearing at about $M = 20$, which corresponds to $\delta y = 0.5$.

4.2 The four-momentum difference, Q^2

The behaviour of the generalised integral BPs for the invariant two-particle squared four-momentum difference, $\chi_q(Q^2)$, is shown in Fig. 6 as a function of $-\ln Q^2$. All BPs, for both data and Monte Carlo, rise with increasing $-\ln Q^2$ (decreasing Q^2). This corresponds to a bunching effect for all orders, similar to the behaviour of fluctuations in y. The anti-bunching effect ($\chi_q(Q^2) < 1$) for small $-\ln Q^2$ is due to energy-momentum conservation [14].

All Monte Carlo models overestimate the $\chi_q(Q^2)$, particularly for large $-\ln Q^2$. A similar discrepancy with JETSET was found for generalised NFMs (so-called density-strip integrals) in Q^2 [21].

Given the large difference in behaviour observed in the previous section between $\eta_2^{(+-)}$ and $\eta_2^{(\pm\pm)}$, we plot in Fig. 7 the behaviour of $\chi_2(Q^2)$ as a function of $-\ln Q^2$ for multiparticle spikes of like- and unlike-charged particles, separately. A significant difference is observed between these two samples. For spikes consisting of particles all having the same charge, a strong bunching effect ($\chi_2^{(\pm\pm)}(Q^2) > 1$) is seen at large $-\ln Q^2$. For unlike-charged particle combinations, the bunching is much smaller and tends to saturate at large $-\ln Q^2$. This latter effect can be explained by resonance decays at intermediate Q^2, since decay products of short-lived resonances tend to be separated in phase space. For like-charged combinations, the resonance effect is much weaker, but BE correlations are expected to contribute. As we see from Fig. 7, JETSET indeed leads to a strong rise of $\chi_2^{(\pm\pm)}(Q^2)$ for like-charged particle combinations, but the influence of BE interference is very small.

It is interesting to observe that JETSET's treatment of the BE correlations does not strongly affect the behaviour of the second-order generalised BP for like-charged combinations, while the second-order BP presented in Figs. 3 and 5 is very sensitive to the BE effect. This comes about because JETSET's modelling of BE interference increases the number of like-sign spikes. This leads to higher values for $\eta_2^{(\pm\pm)}$. However, χ_2 is mainly influenced by the shape of the spike-multiplicity distribution rather than by the average spike multiplicity.

As in the case of the rapidity measurements in section 4.1, all Monte Carlo models overestimate the data for unlike-charged combinations. As seen from the large (systematic) errors for $-\ln Q^2 > 3$, the JETSET predictions are highly sensitive to the parameters of the Lund string fragmentation.

5 Conclusions

For the first time, local multiplicity fluctuations of experimental data have been studied by means of bunching parameters. Using this technique, fluctuations in rapidity defined with respect to the thrust axis are found to exhibit multifractal behaviour.

The power-law behaviour of second-order BPs is mainly due to like-charged particles. JETSET gives the same power-law trend even without the BE effect. This means that the power law observed for like-charged particles appears to be largely a consequence of parton showers and hadronisation.

Although Monte Carlo models describe well the inclusive rapidity and Q^2 distributions, they fail to describe fluctuations in these variables as measured by the bunching parameters. It appears that some important points in the simulation of hadronisation and resonance production as well as a correct simulation of the BE effect are missing in these models.

Acknowledgements

We wish to express our gratitude to the CERN accelerator divisions for the excellent performance of the LEP machine. We acknowledge the effort of all engineers and technicians who have participated in the construction and maintenance of this experiment. We thank V. I. Kuvshinov, J.-L. Meunier and R. Peschanski for useful discussions and comments.

References

[1] A. Białas and R. Peschanski, Nucl. Phys. **B273** (1986) 703; Nucl. Phys. **B308** (1988) 857.

[2] P. Bożek, M. Płoszajczak and R. Botet, Phys. Rep. **252** (1995) 101;
E.A. De Wolf, I.M. Dremin and W. Kittel, Phys. Rep. **270** (1996) 1.

[3] TASSO Collab., W. Braunschweig *et al.*, Phys. Lett. **B231** (1989) 548.

[4] K. Sugano (HRS Collab.), Proc. Santa Fe Workshop "Intermittency in High-Energy Collisions", Eds.: F. Cooper *et al.* (World Scientific, Singapore, 1991) p.1.

[5] CELLO Collab., H.J. Behrend *et al.*, Phys. Lett. **B256** (1991) 97.

[6] DELPHI Collab., P. Abreu *et al.*, Phys. Lett. **B247** (1990) 137;
A. De Angelis, Mod. Phys. Lett. **A5** (1990) 2395.

[7] OPAL Collab., M.Z. Akrawy *et al.*, Phys. Lett. **B262** (1991) 351.

[8] ALEPH Collab., D. Decamp *et al.*, Z. Phys. **C53** (1992) 21.

[9] DELPHI Collab., P. Abreu *et al.*, Nucl. Phys. **B386** (1992) 471.

[10] L3 Collab., B. Adeva *et al.*, Z. Phys. **C55** (1992) 39.

[11] F. Mandl and B. Buschbeck (DELPHI Collab.), Proc. 24 Int. Symp. on Multiparticle Dynamics, Vietri sul Mare (Italy), 1994, Eds.: A. Giovannini *et al.* (World Scientific, Singapore, 1995) p.52;
B. Buschbeck and F. Mandl, ICHEP'96 Ref. pa01-028;
B. Buschbeck, P. Lipa, F. Mandl (DELPHI Collab.), Proc. 7th Int. Workshop on Multiparticle Production "Correlations and Fluctuations", Nijmegen, The Netherlands 1996, Eds.: R.C. Hwa *et al.* (World Scientific, Singapore, 1997) p.175.

[12] E.M. Friedlander, Mod. Phys. Lett. **A4** (1989) 2457;
W.Kittel, Proc. Santa Fe Workshop "Intermittency in High-Energy Collisions", Eds.: F.Cooper *et al.* (World Scientific, Singapore, 1991) p.83;
P.Lipa *et al.*, Z. Phys. **C54** (1992) 115.

[13] S.V. Chekanov and V.I. Kuvshinov, Acta Phys. Pol. **B25** (1994) 1189;
S.V. Chekanov, W. Kittel and V.I. Kuvshinov, Acta Phys. Pol. **B27** (1996) 1739.

[14] S.V. Chekanov, W. Kittel and V.I. Kuvshinov, Z. Phys. **C74** (1997) 517.

[15] A. Białas and M. Gazdzicki, Phys. Lett. **B252** (1990) 483;
W. Ochs, Z. Phys. **C50** (1991) 339.

[16] P. Grassberger, Phys. Lett. **A 97** (1983) 227;
H. Hentschel, I. Procaccia, Physica **D8** (1983) 43.

[17] L3 Collab., B. Adeva *et al.*, Nucl. Instr. Meth. **A289** (1990) 35; J.A. Bakken *et al.*, Nucl. Instr. Meth. **A275** (1989) 81; O. Adriani *et al.*, Nucl. Instr. Meth. **A302** (1991) 53; B. Adeva *et al.*, Nucl. Instr. Meth. **A323** (1992) 109; K. Deiters *et al.*, Nucl. Instr. Meth. **A323** (1992) 162; B. Acciari *et al.*, Nucl. Instr. Meth. **A351** (1994) 300.

[18] R. Brun *et al.*, CERN report CERN DD/EE/84-1 (Revised), 1987.

[19] H. Fesefeldt, RWTH Aachen report PITHA 85/02, 1985.

[20] S.V. Chekanov, "Local Multiplicity Fluctuations and Intermittent Structure Inside Jets", Ph.D. Thesis, Univ. of Nijmegen, The Netherlands 1997.

[21] A.A. Syed, "Particle Correlations in Hadronic Decays of the Z Boson", Ph.D. Thesis, Univ. of Nijmegen, The Netherlands 1994.

[22] T. Sjöstrand, Comp. Phys. Comm. **82** (1994) 74.

[23] L. Lönnblad, Comp. Phys. Comm. **71** (1992) 15.

[24] G. Marchesini and B.R. Webber, Nucl. Phys. **B310** (1988) 461;
G. Marchesini *et al.*, Comp. Phys. Comm. **67** (1992) 465.

[25] Sunanda Banerjee and Swagato Banerjee, L3 Note 1978 (1996);
I.G. Knowles and T. Sjöstrand (conveners), "QCD Event Generators", Physics at LEP2, CERN-96-01, Vol. 2 (1996) p.103.

[26] ALEPH Collab., D. Buskulic *et al.*, Z. Phys. **C69** (1995) 15.

[27] B. Andersson, G. Gustafson, G. Ingelman, T. Sjöstrand, Phys. Rep. **97** (1983) 31.

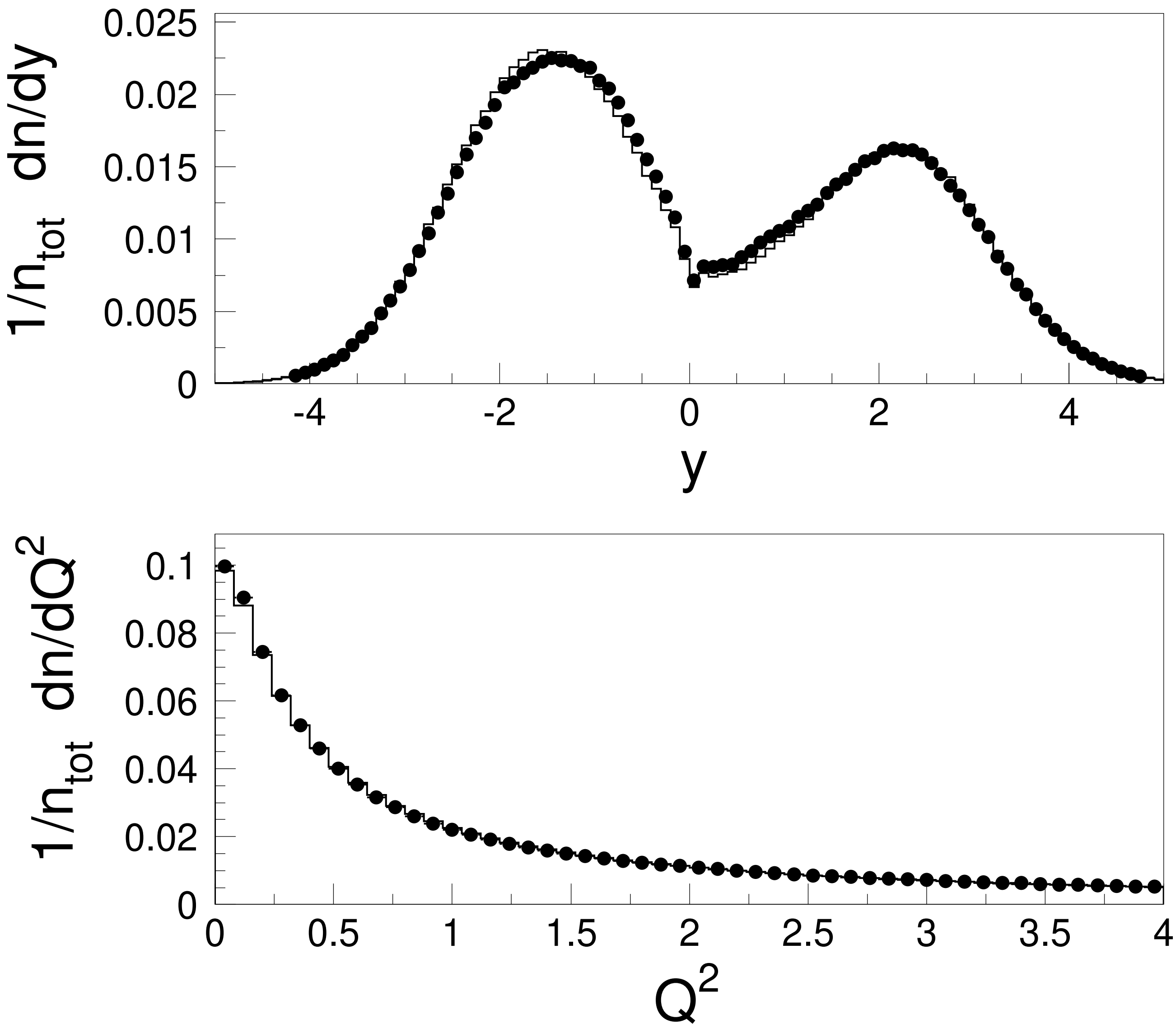

Figure 1: Distributions of the single-particle rapidity with respect to the thrust axis, y, and the inclusive four-momentum difference squared, Q^2, for uncorrected data (points) compared to the predictions of JETSET after detector simulation (histogram).

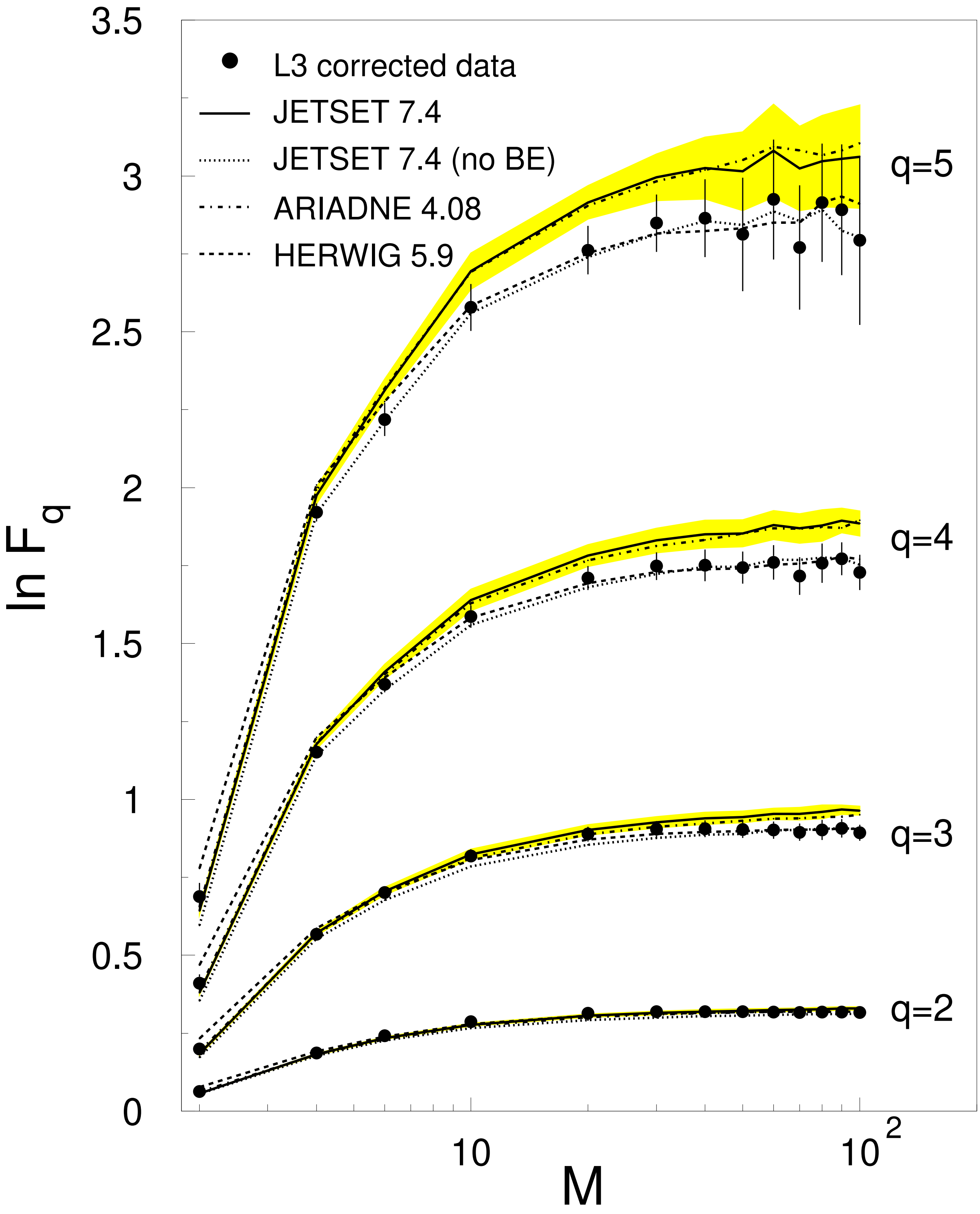

Figure 2: NFMs as a function of the number of bins, M, in the transformed rapidity defined with respect to the thrust axis. The shaded areas represent the errors on the JETSET predictions. The errors on the ARIADNE predictions are comparable whereas those on the HERWIG predictions are about 50% larger.

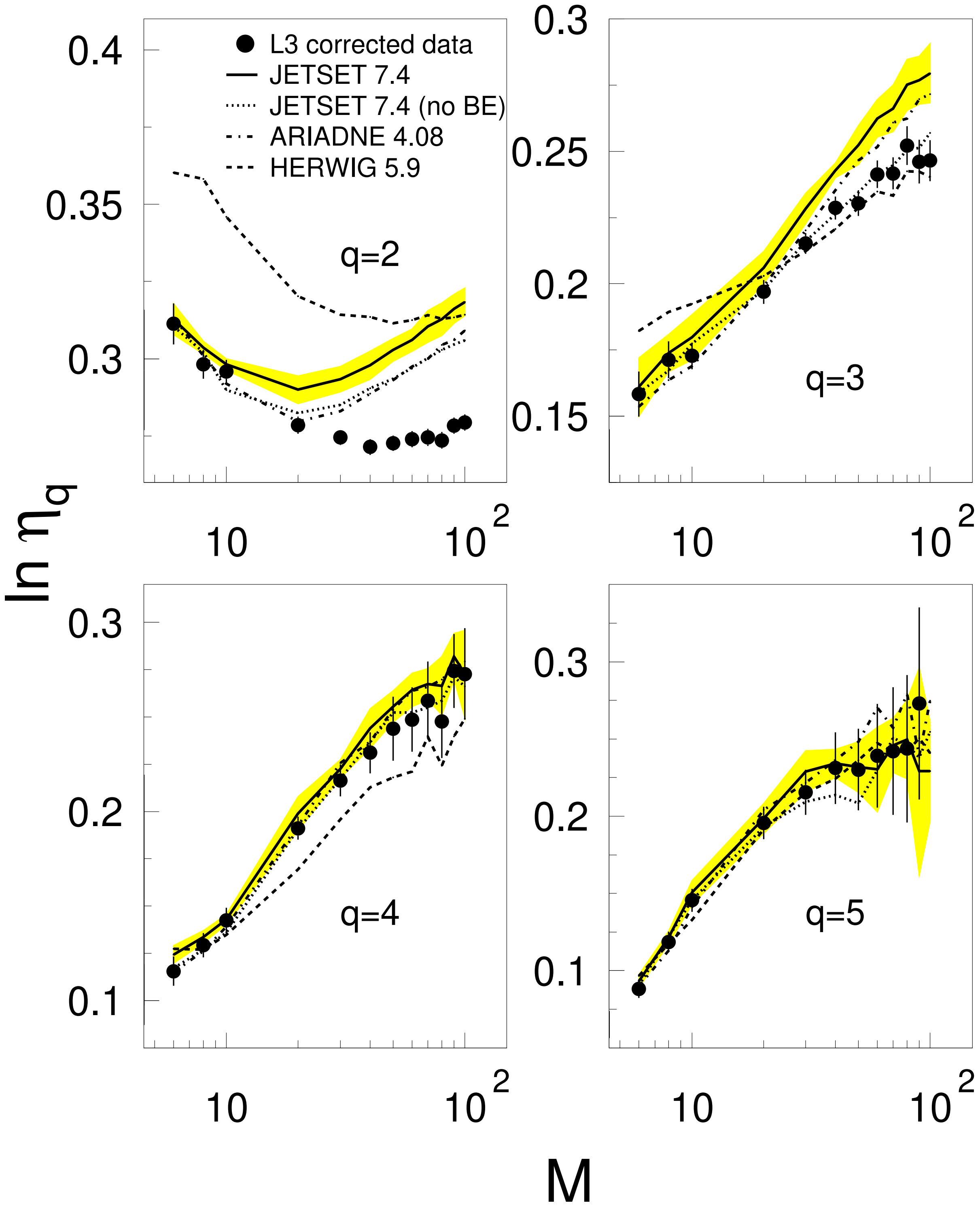

Figure 3: BPs as a function of the number of bins, M, in the transformed rapidity defined with respect to the thrust axis. The shaded areas represent the errors on the JETSET predictions. The errors on the ARIADNE predictions are comparable whereas those on the HERWIG predictions are about 50% larger.

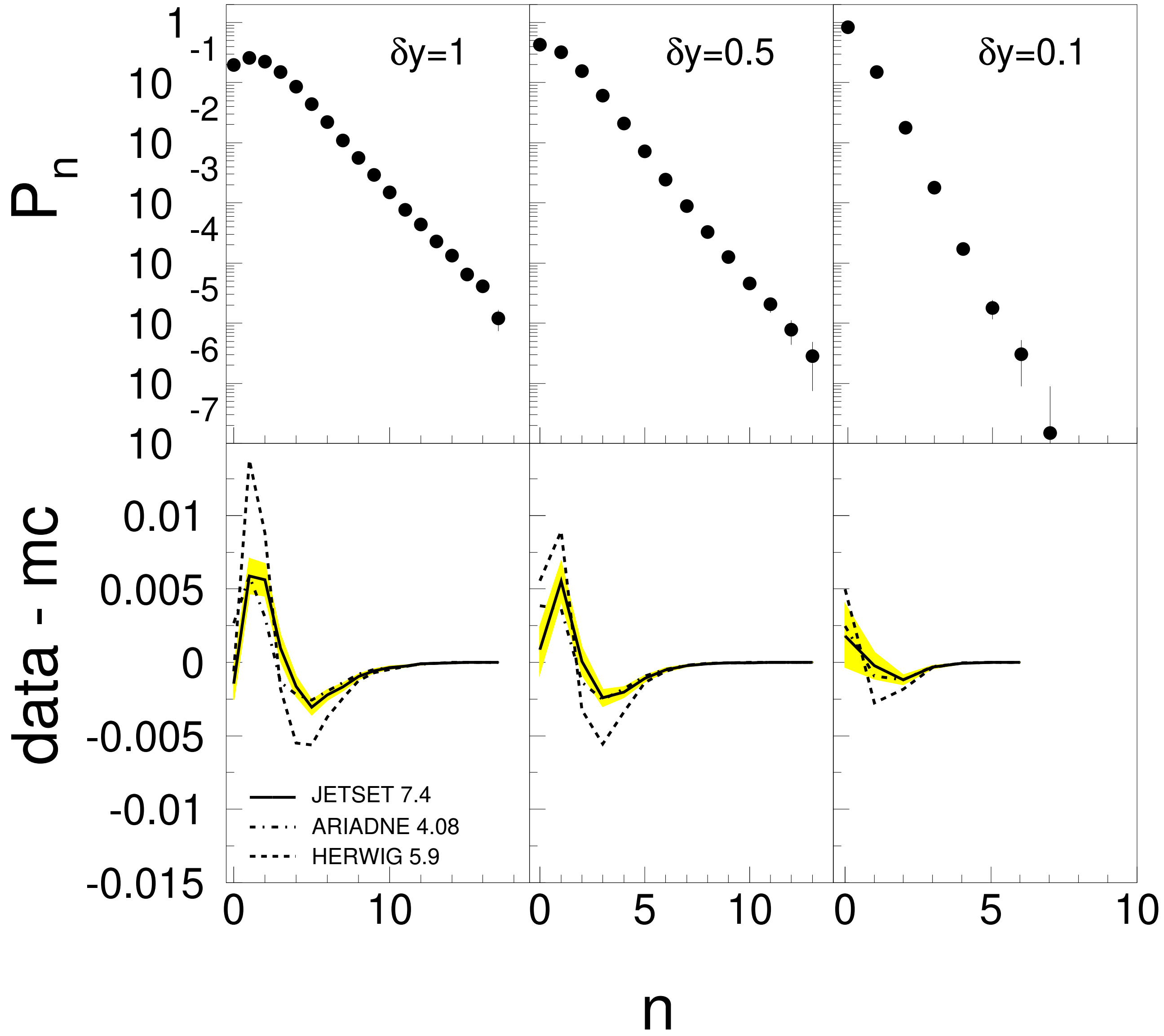

Figure 4: The multiplicity distribution in bins of rapidity with respect to the thrust axis, $P_n(\delta y)$, for $\delta y = 1.0$, 0.5, 0.1 ($M = 10$, 20, 100). The shaded areas represent the errors on the JETSET predictions. The errors on the ARIADNE predictions are comparable whereas those on the HERWIG predictions are about 50% larger.

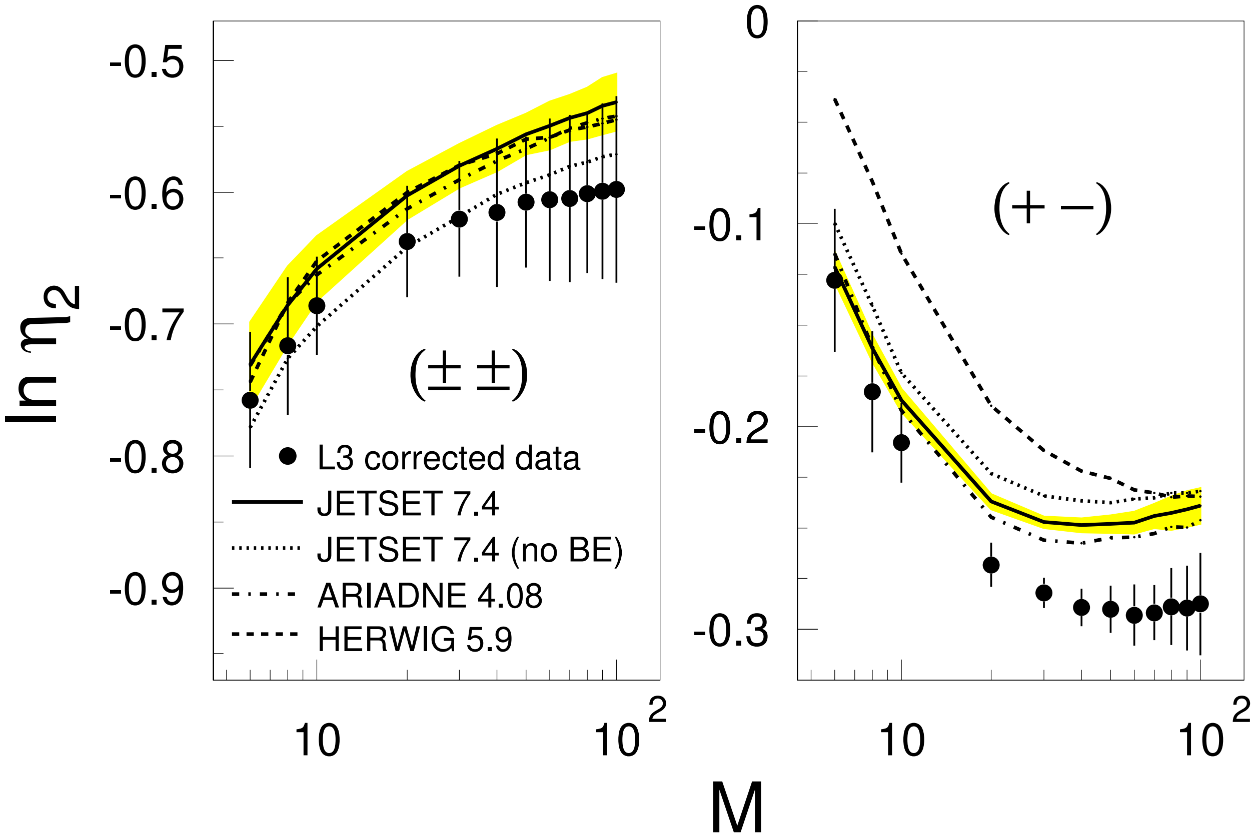

Figure 5: The second-order BP as a function of the number of bins, M, in the transformed rapidity defined with respect to the thrust axis for like-charged and unlike-charged particle combinations. The shaded areas represent the errors on the JETSET predictions. The errors on the ARIADNE predictions are comparable whereas those on the HERWIG predictions are about 50% larger.

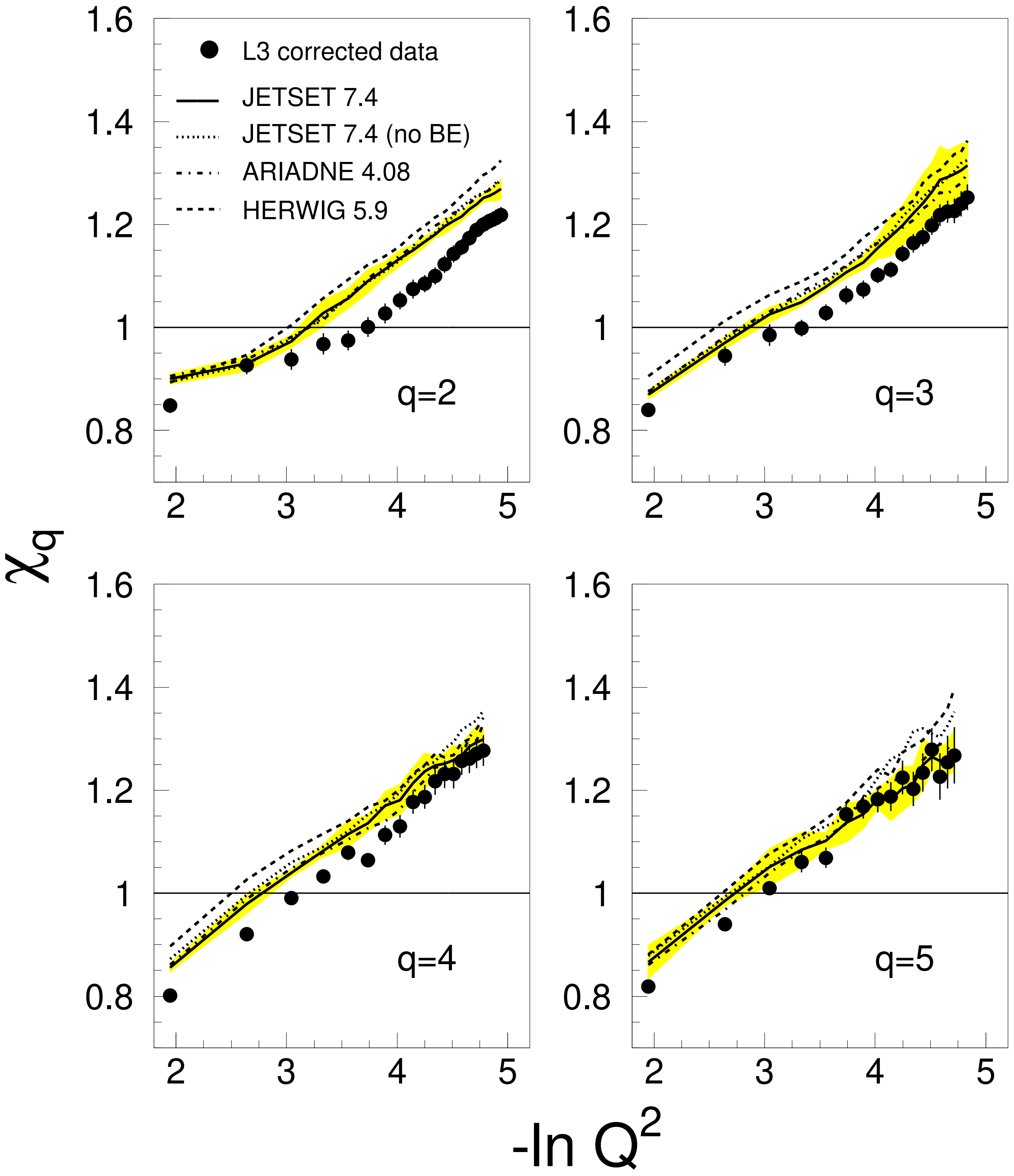

Figure 6: Generalised integral BPs as a function of the squared four-momentum difference $Q^transformed2$ in GeV^2 between two charged particles. The shaded areas represent the errors on the JETSET predictions. The errors on the ARIADNE predictions are comparable whereas those on the HERWIG predictions are about 50% larger.

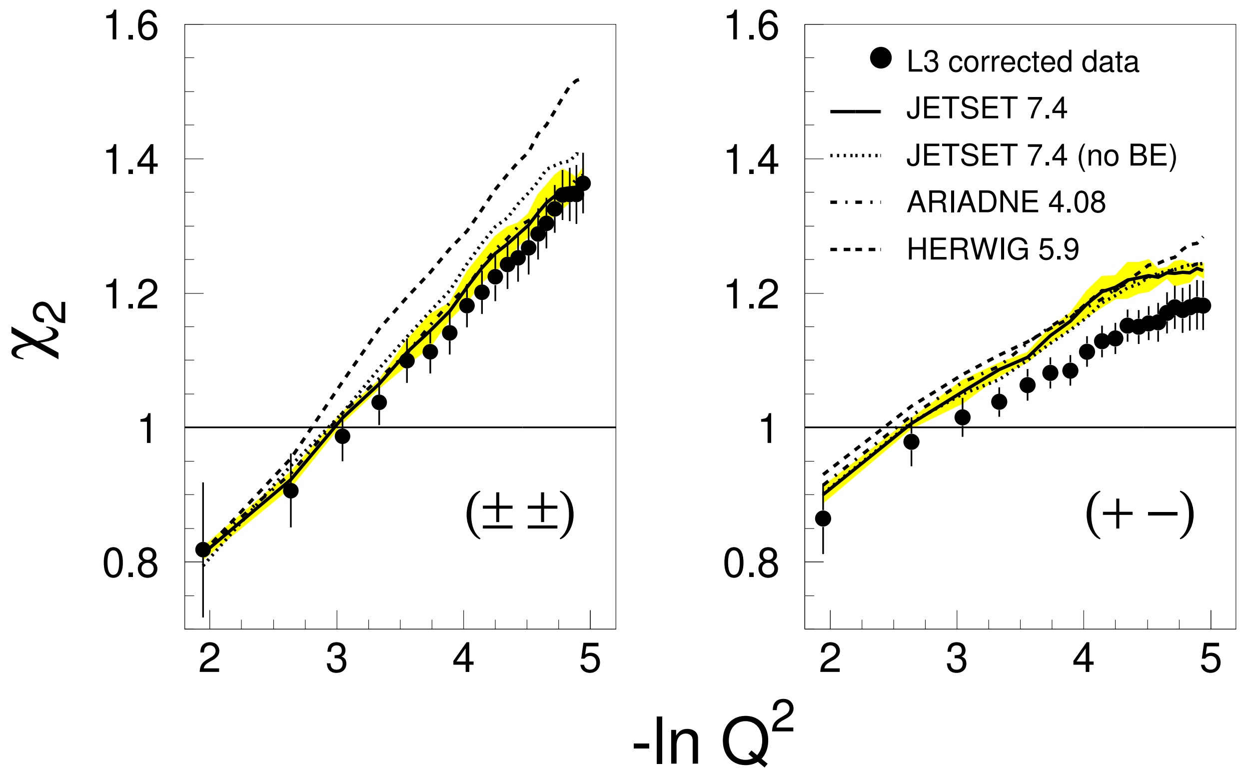

Figure 7: Generalised second-order BP as a function of the squared four-momentum difference Q^2 in GeV^2 between two charged particles for like-charged and unlike-charged particle combinations. The shaded areas represent the errors on the JETSET predictions. The errors on the ARIADNE predictions are comparable whereas those on the HERWIG predictions are about 50% larger.